Investigation of Atomic Displacements at a $\Sigma 3$ {111} Twin Boundary in $BaTiO_3$ by Means of Phase-Retrieval Electron Microscopy

C. L. Jia and A. Thust

Institut für Festkörperforschung, Forschungszentrum Jülich GmbH, D-52425, Jülich, Germany

(Received 22 December 1998)

We applied the technique of focal-series reconstruction in high-resolution electron microscopy for a precise determination of the spacings between atomic columns at a $\Sigma 3$ {111} twin boundary in perovskite $BaTiO_3$. We succeeded in observing a predicted expansion of the nearest Ti-Ti spacing across the boundary plane and found additionally a contraction of the nearest BaO-BaO spacing. Moreover, the direct visualization of oxygen columns in the boundary plane is demonstrated. The boundary structure agrees in detail with a subunit of the hexagonal phase of $BaTiO_3$. [S0031-9007(99)09438-7]

PACS numbers: 61.16.Bg, 42.30.Rx, 61.72.Mm

It is well known that high-resolution transmission electron microscopy (HRTEM) images suffer from nonlinear contrast artifacts, from gaps in the range of spatial frequencies transmitted, and from severe optical aberrations introduced by the objective lens of the microscope. Such effects often hamper a direct image analysis and require extensive image simulations in order to determine the underlying object structure [1]. Among the manifold unwanted contrast phenomena, the distances between aperiodic object features are, in general, also imaged incorrectly.

In contrast to the common approach of determining interatomic spacings from one single high-resolution micrograph either by direct measurement [2] or indirect refinement methods [3], our investigation is based on the phase of the electron wave function which is numerically reconstructed from a series of images taken at different objective lens defocus values [4–7]. The electron wave function at the exit plane of the object (exit-plane wave function, EPW) is almost free of the above-mentioned optical artifacts and exhibits a signal-to-noise ratio which is far better than that of a single input image [8]. Apart from a dramatic simplification of the contrast interpretation, systematic as well as statistical errors related to local distance measurements can be substantially reduced by using the reconstruction technique.

In this Letter we report on the use of the focal-series reconstruction technique in HRTEM for high-precision measurements of interatomic distances at a $\Sigma 3$ {111} twin boundary in a thin film of $BaTiO_3$. The boundary plane of $\Sigma 3$ {111} twins in bulk material was identified as a {111} Ba-O_3 plane [9]. Oxygen octahedra located at the boundary share a common face, forming Ti_2O_9 groups. Such Ti_2O_9 groups are also a basic structural feature of the hexagonal phase of $BaTiO_3$, which is stable at high temperatures above 1325 °C [10]. In the hexagonal structure the repulsion between the Ti atoms causes a shift of the Ti atoms out of their ideal octahedral center position leading to an expansion of the Ti-Ti spacing from 0.234 to 0.267 nm [11]. Therefore, a similar expansion of the Ti-Ti spacing across the {111} twin boundary plane was expected by Eibl *et al.* [12]. However, an HRTEM study on twin boundaries in bulk material did not confirm such an expansion [9].

The samples investigated in the present work are $BaTiO_3$ thin films grown on $Pt/Ti/SiO_2/Si$ wafers by the pulsed-laser deposition technique [13]. High-resolution imaging was performed on a Philips CM20ST FEG electron microscope operated at 200 kV. A series of 20 images was recorded from a plan-view sample with a 1024×1024 pixels slow-scan charge coupled device camera at a spatial sampling rate of 0.0248 nm/pixel. The 20 images were recorded from the same object area with an equidistant focal decrement of -5.3 nm between successive exposures. In order to measure all relevant anisotropic aberrations of the objective lens (coma, two-, and threefold astigmatism) as they were present at the time of data acquisition, a tilt-azimuth series of 16 images was recorded shortly after the acquisition of the focal series from an amorphous region adjacent to the area of interest [14].

The numerical reconstruction of the EPW was carried out using the Philips/Brite-Euram focal-series reconstruction package [7]. The EPW was retrieved in the spatial frequency band between 1 and 6.5 nm^{-1}, corresponding to a real-space length range between 1 and 0.15 nm. After reconstruction and correction for the measured optical aberrations, the complex-valued EPW was split into amplitude and phase. Since for thin specimens most of the relevant information is stored in the phase of the EPW, and for reasons of compactness, only the phase information will be treated in this Letter. In order to identify phase maxima of different heights with the correct atomic species, EPWs for various specimen thickness values were simulated as a reference basis using the EMS program package [1].

Figures 1(a) and 1(b) show, as typical examples of the complete focal series, two high-resolution images of the twin boundary region. The images appear blurred over

 0031-9007/99/82(25)/5052(4)$15.00

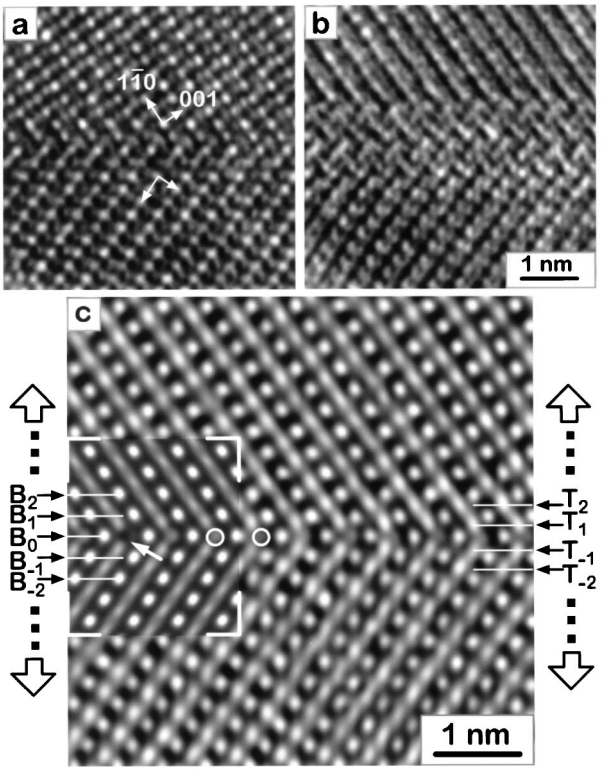

FIG. 1. (a) and (b) Two high-resolution images of a $\Sigma 3$ {111} twin boundary in perovskite $BaTiO_3$ viewed along a ⟨110⟩ zone axis. The images belong to a focal series of 20 images and were taken at defocus values of −183 and −262 nm. (c) Phase of EPW reconstructed from the focal series. The inset at the left is a simulation for a specimen thickness of 2.8 nm. Circles denote oxygen columns located in the boundary plane. The arrow marks a position, where oxygen has been intentionally omitted from the simulation model. {111} Ti planes are labeled with "*T*" and {111} Ba-O planes with "*B*".

a radius of several nanometers and cannot be used for a direct interpretation. The massive blurring is caused by the spherical aberration of the objective lens in combination with the improved coherence properties offered by field-emission electron guns (FEG). In Fig. 1(c) the phase of the reconstructed EPW is displayed for comparison. Note that the strong blurring effect, which is typical of the newest generation of FEG microscopes, is no longer recognizable in the reconstructed phase. The inset marked by white corners in Fig. 1(c) is a simulation of the phase for a sample thickness of 2.8 nm. According to the simulation, the prominent maxima in the phase image coincide with Ba-O columns viewed along the [110] direction. A second type of a comparatively less prominent phase maximum is located at the position of the Ti columns, and the faint streaks connecting these less prominent phase maxima arise from oxygen columns located in between the Ti columns.

Because of the extremely low contrast, the possibility of a direct observation of oxygen columns by means of high-resolution electron microscopy has often been discussed. As a consequence of the improved signal-to-noise ratio of the reconstructed EPW one can directly observe oxygen columns located in the boundary plane as weak phase maxima, as is marked by circles in Fig. 1(c). The possibility that the weak maxima are not due to oxygen can be ruled out by means of EPW simulations. An arrow in the simulated phase image denotes a test position, where a single oxygen column has been intentionally omitted from the structure model entering the simulation. Exactly at that specific test position, the weak maximum disappears from the simulated phase, as is expected. The fact that oxygen shows up directly only in the boundary plane is due to the limited resolution of the microscope which is not sufficient for imaging the bulk Ti-O distance.

The analysis of the phase image of Fig. 1(c) was carried out in a three-step procedure. First, the coordinates of the single phase maxima, which represent single atomic columns, were determined with subpixel accuracy using a center-of-gravity approach. Second, distances between such phase maxima were determined, either across or parallel to the boundary plane. Third, equivalent distances between maxima, which are invariant with respect to a translation parallel to the boundary plane, were averaged in order to obtain an additional statistical improvement of the length measurements.

The {111} Ti planes and {111} Ba-O planes follow an alternating stacking sequence in a direction perpendicular to the boundary and are denoted in the following by "*T*" and "*B*," respectively. We number these atomic planes by indexing the central Ba-O boundary plane as B_0. Subsequently, moving away from the boundary, the Ti planes T_n $(n = \pm 1, 2, 3, \ldots)$ follow alternating with the Ba-O planes B_n $(n = \pm 1, 2, 3, \ldots)$. Distances perpendicular to the boundary plane were measured with respect to the common reference plane B_0 and are compared to the ideal geometrical model of a twin boundary exhibiting equidistant {111} plane spacings.

Figures 2(a) and 2(b) show the average displacement δ_a of the phase maxima in various *T* and *B* planes from their geometrically ideal position in a direction perpendicular to the boundary plane. Positive values represent a displacement away from the boundary plane (expansion) and negative values denote a displacement towards the boundary plane (contraction).

Although imaging artifacts can be widely eliminated in the reconstructed EPW, the maximum positions determined directly from the phase image still do not coincide exactly with the true atomic column positions, but depend slightly on the spatial resolution at which the EPW is retrieved. Figure 3 shows a comparison between the real interatomic displacements δ_r underlying a simple simulation model (a) and the resulting apparent displacements δ_a determined from phase images simulated for a resolution of 0.1 (b) and 0.15 nm (c). A systematic deviation of the apparent displacements δ_a from the real displace-

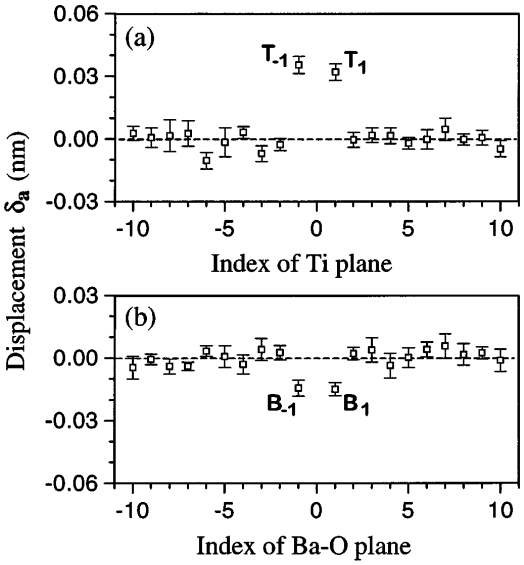

FIG. 2. Apparent displacements δ_a of atomic columns belonging to (a) {111} Ti planes and (b) {111} Ba-O planes as determined from the phase of the reconstructed EPW. Positive values indicate a larger, negative values a smaller distance to the boundary plane when compared to a model with fixed {111} plane spacings. For the indexing scheme, see Fig. 1. The error bars indicate a statistical confidence level of 95%.

ments δ_r occurs for a resolution of 0.15 nm, which is the information limit of the microscope in use. The observed discrepancy is due to the fact that any resolution-limited observation technique produces data which are spatially convoluted with a point-spread function corresponding to the frequency cutoff in diffraction space. The tails of the point-spread function emerging from the boundary plane can be observed equally well in the experimental data of Fig. 2 and in the test simulations of Fig. 3(c). As is shown in Fig. 3(b), the systematic distortions are substantially reduced for an instrumental information limit of 0.1 nm. Because of the 0.15 nm information limit of our microscope we have to employ a refinement procedure to determine the true interatomic spacings with the highest possible accuracy. For this purpose the atomic positions of a model structure are slightly readjusted in such a way that the apparent displacements δ_a of the resulting simulated phase image match the apparent displacements δ_a of the experimentally reconstructed phase within the experimental error bars.

Figures 4(a) and 4(c) display the best fit obtained for the apparent displacements δ_a of the atomic columns in the various T and B planes on the assumption that the twin boundary has a mirror symmetry, whereas Figs. 4(b) and 4(d) show the underlying real displacements δ_r. The largest real displacement of $\delta_r = +0.019$ nm is observed for the atomic columns in the $T_{\pm 1}$ planes. The positive value denotes an expansion and reflects an increased Ti-Ti spacing across the boundary of 0.270 ± 0.004 nm. The Ba-O columns in the $B_{\pm 1}$ planes are displaced by $\delta_r = -0.016$ nm towards the boundary plane B_0, reflecting a contraction to a spacing of 0.216 ± 0.004 nm. A model of the twin boundary viewed along a $\langle 110 \rangle$ direction is shown in Fig. 5(a). As is shown in Figs. 4(b) and 4(d), considerably smaller real displacements ($\delta_r \leq 0.005$ nm) have been measured for the columns in the planes $B_{\pm 2,3,4}$ and $T_{\pm 2,3,4}$. The values determined are already in the

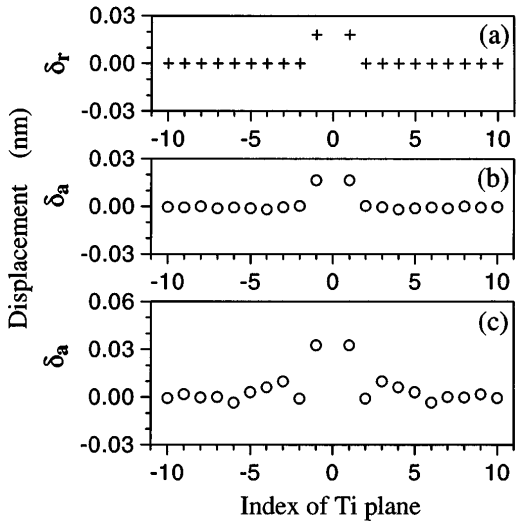

FIG. 3. (a) Real displacements δ_r of Ti atoms in various {111} planes entering a simulation model of a mirror symmetric twin boundary (input). (b) Apparent displacements δ_a as determined from the phase of the resulting EPW for a sample thickness of 2.8 nm and a resolution of 0.1 nm (output). (c) Same as (b), but for a resolution of 0.15 nm.

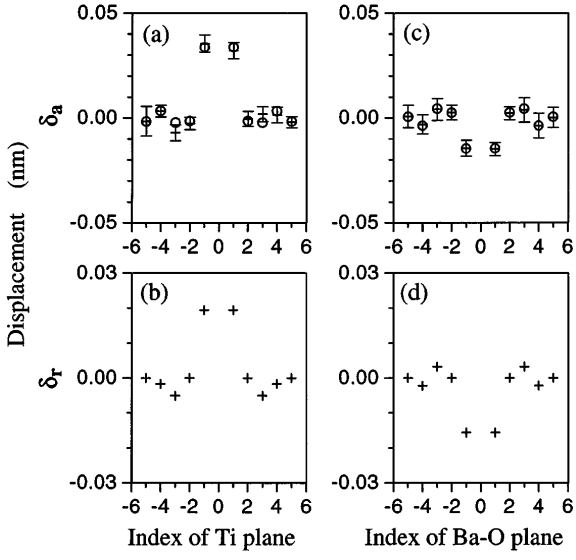

FIG. 4. Best correspondence between apparent displacements δ_a determined from the experimental EPW reconstruction (dashed with error bars) and those resulting from EPW simulations (open circles) of a symmetric boundary for (a) Ti columns and (c) Ba-O columns. The underlying real displacements δ_r are shown in (b) and (d). The experimental error bars indicate a statistical confidence level of 95%.

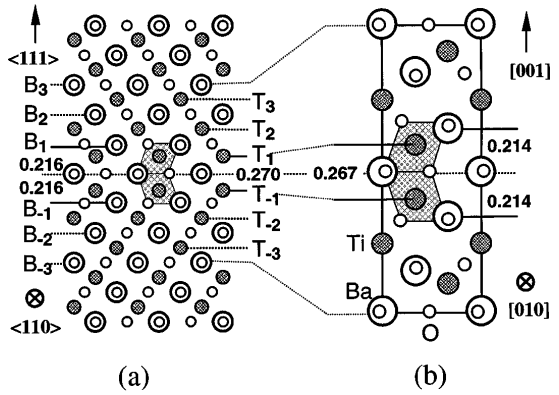

FIG. 5. (a) Schematic drawing of a {111} twin boundary in perovskite $BaTiO_3$ viewed along a ⟨110⟩ direction. (b) Unit cell of hexagonal $BaTiO_3$ projected along the [010] direction. Ti_2O_9 groups are marked by shaded rhombuses.

order of the statistically determined measurement error and are thus of low significance.

The possible existence of atomic column displacements in a direction parallel to the boundary plane has also been investigated for the atomic columns in the $B_{0,\pm1}$ and $T_{\pm1}$ planes, yielding real displacements δ_r smaller than 0.005 nm, which are again of low statistical significance.

We were able to experimentally confirm the predicted expansion of the Ti-Ti spacing across {111} twin boundaries of the room temperature phase of $BaTiO_3$. Forming a twin boundary model under purely geometrical considerations, the Ti-Ti spacing across a twin boundary has to be substantially reduced from the bulk spacing of the Ti ions of 0.401 nm [15] towards the bulk spacing of the {111} planes of 0.232 nm, leading to a strong repulsion. This expansion was also expected from the repulsion between the Ti^+ ions in the Ti_2O_9 groups of the hexagonal structure [12].

We additionally observe a reduction of the spacing between the planes $B_{\pm1}$ and B_0. This finding is consistent in detail with the atomic configuration of the hexagonal phase which is displayed in Fig. 5(b) along the [010] viewing direction. It can be seen that a hexagonal unit cell includes two antioriented Ti_2O_9 groups which also occur at the {111} twin boundary of the perovskite matrix. For the Ti-Ti spacing across the boundary we determined a value of 0.270 nm, which agrees within the measurement error with the value of 0.267 nm belonging to the hexagonal phase. Similarly, the spacing of 0.216 nm between the boundary Ba-O plane and the neighboring Ba-O planes matches the hexagonal value of 0.214 nm. Based on this structural similarity one can conclude that the atomic spacings in the twin boundary area tend to relax towards the low energy configuration of the hexagonal unit cell.

By the use of the reconstruction technique we successfully reduced the drastic point spread affecting the input images, extending over several nanometers, to a value near 0.15 nm, which corresponds to the information limit of the microscope in use. The residual geometrical distortions observed in the phase of the reconstructed EPW are in our case only around 0.02 nm and cannot be avoided due to the limited resolution of the microscope. In order to achieve a measurement accuracy even better than 0.02 nm, a refinement procedure had to be employed additionally. A future development of microscopes with an information limit of 0.1 nm or less would be of great advantage, because then such measurements could in many cases be performed directly on the reconstructed EPW without an extra refinement step.

The authors are grateful to R. Rosenfeld, M. Lentzen, and K. Urban for fruitful discussions and comments.

[1] P. A. Stadelmann, Ultramicroscopy **21**, 131 (1987).
[2] R. Bierwolf *et al.*, Ultramicroscopy **49**, 273 (1993).
[3] O. Kienzle *et al.*, J. Microsc. **190**, 144 (1998).
[4] W. Coene *et al.*, Phys. Rev. Lett. **69**, 3743 (1992).
[5] W. M. J. Coene *et al.*, Ultramicroscopy **64**, 109 (1996).
[6] M. Op de Beeck, D. Van Dyck, and W. Coene, Ultramicroscopy **64**, 167 (1996).
[7] A. Thust *et al.*, Ultramicroscopy **64**, 211 (1996).
[8] A. Thust and R. Rosenfeld in *Proceedings of the 14th International Congress on Electron Microscopy, Cancun, Mexico, 1998* (Institute of Physics Publishing, Bristol/Philadelphia, 1998), Vol. 1, p. 119.
[9] A. Recnik *et al.*, Philos. Mag. B **70**, 1021 (1994).
[10] H. Arend and L. Kihlborg, J. Am. Ceram. Soc. **52**, 63 (1969).
[11] R. D. Burbank and H. T. Evans, Jr., Acta Crystallogr. **1**, 330 (1948).
[12] O. Eibl, P. Pongratz, and P. Skalicky, Philos. Mag. B **57**, 521 (1987).
[13] M. Mertin, Ph.D. thesis, RWTH, Aachen, 1996.
[14] A. Thust *et al.*, Ultramicroscopy **64**, 249 (1996).
[15] H. D. Megaw, Proc. R. Soc. London A **189**, 261 (1947).